JOURNAL OF ENVIRONMENTAL SCIENCES 100 (2021) 279–286

Available online at www.sciencedirect.com

ScienceDirect

www.elsevier.com/locate/jes

JES JOURNAL OF ENVIRONMENTAL SCIENCES

www.jesc.ac.cn

Humidity and $PM_{2.5}$ composition determine atmospheric light extinction in the arid region of northwest China

Xiaoxiao Zhang[1], *Xiang Ding*[2,3], *Dilinuer Talifu*[1,*], *Xinming Wang*[2,3], *Abulikemu Abulizi*[1], *Mailikezhati Maihemuti*[1], *Suwubinuer Rekefu*[1]

[1] *Key Laboratory of Coal Clean Conversion and Chemical Engineering Process, Xinjiang Uyghur Autonomous Region, Xinjiang University, Urumqi 830046, China*

[2] *State Key Laboratory of Organic Geochemistry, Guangzhou Institute of Geochemistry Chinese Academy of Sciences, Guangzhou 510640, China*

[3] *Guangdong-Hong Kong-Macao Joint Laboratory for Environmental Pollution and Control, Guangzhou 510640, China*

ARTICLE INFO

Article history:
Received 12 February 2020
Revised 2 July 2020
Accepted 6 July 2020
Available online 14 August 2020

Keywords:
Aerosol chemical composition
Visibility
IMPROVE
Light extinction
Source apportionment
South of Urumqi

ABSTRACT

Atmospheric visibility can directly reflect the air quality. In this study, we measured water-soluble ions (WSIs), organic and element carbon (OC and EC) in $PM_{2.5}$ from September 2017 to August 2018 in Urumqi, NW China. The results show that SO_4^{2-}, NO_3^- and NH_4^+ were the major WSIs, together accounting for 7.32%–84.12% of $PM_{2.5}$ mass. Total carbon (TC=OC+EC) accounted for 12.12% of $PM_{2.5}$ mass on average. And OC/EC > 2 indicated the formation of secondary organic carbon (SOC). The levels of SO_4^{2-}, NO_3^- and NH_4^+ in low visibility days were much higher than those in high visibility days. Relative humidity (RH) played a key role in affecting visibility. The extinction coefficient (b_{ext}) that estimated via Koschmieder formula with visibility was the highest in winter (1441.05 ± 739.95 Mm^{-1}), and the lowest in summer (128.58 ± 58.00 Mm^{-1}). The b_{ext} that estimated via IMPROVE formula with $PM_{2.5}$ chemical component was mainly contributed by $(NH_4)_2SO_4$ and NH_4NO_3. The b_{ext} values calculated by both approaches presented a good correlation with each other (R^2 = 0.87). Multiple linear regression (MLR) method was further employed to reconstruct the empirical regression model of visibility as a function of $PM_{2.5}$ chemical components, NO_2 and RH. The results of source apportionment by Positive Matrix Factorization (PMF) model showed that residential coal combustion and vehicle emissions were the major sources of b_{ext}.

Introduction

Air pollution in China has become serious owing to the rapid development of economy, industrialization and urbanization. A series of $PM_{2.5}$ pollution events arouse worldwide attention. The chemical composition of $PM_{2.5}$ is extremely complex and mainly composed of water-soluble ions, organic matter, black carbon, and heavy metals. $PM_{2.5}$ not only has adverse effect on human health (Palomo, 1999; Raizenne et al., 1996; Pope et al., 2009) but also directly or indirectly affects atmospheric chemistry, visibility, acid deposition, cloud and pre-

* Corresponding author.
E-mail: dilnurt@xju.edu.cn (D. Talifu).

https://doi.org/10.1016/j.jes.2020.07.007
1001-0742/

cipitation formation as well as radiation balance (Zhang et al., 2012; Kaufman et al., 2002; Liu et al., 1999).

In recent decades, haze events frequently happened in China's urban areas, with $PM_{2.5}$ concentrations largely exceeding the national standard (Tan et al., 2016; Zhang et al., 2011, 2017; Jun et al., 2015). Low visibility is associated with high concentrations of suspended particles, especially fine particles (< $PM_{1.0}$). The absorbing aerosol has a large Ångström exponent (AAE) value, 1.58 at 470/660 nm, much large than the scattering aerosols (SAE) (Zhuang et al., 2017). The chemical composition, size and concentration of particle matter in the atmosphere affect visibility. Zou et al. (2018) found that ~30% of the light extinction coefficient came from secondary aerosols. Many previous studies have found that SO_4^{2-}, NO_3^- and black carbon in $PM_{2.5}$ aerosol have strong scattering and absorbing effects (Lowenthal and Kumar, 2012; Hand et al., 2002; Kim et al., 2001; Chen and Bond, 2009; Pathak et al., 2009; Wu et al., 2017a). In addition, other species in aerosols also have an impact on visibility. Wang et al. (2018) studied the atmospheric particle of the Tibetan plateau and found that rBC (refractory Black Carbon) had strong light absorption properties, and the rBC coated on particles was positively correlated with the light absorption intensity. The total light absorption contribution of brown carbon to aerosol could reach 20–40% at the wavelength of 350 nm, indicating that the light absorption contribution of brown carbon in the short-wave region cannot be ignored (Chen and Bond, 2009). However, BC is not the only particle that absorbs sunlight, humus, humus-like substances and bio-aerosols have also been verified as sunlight absorbing particles (Andreae and Gelencsér, 2006). The hygroscopicity of water-soluble substances in $PM_{2.5}$ (mainly including water-soluble ions, water-soluble organic carbon and inorganic carbon) has a negative impact on visibility.

At present, the research on the optical characteristics and chemical components of particle in China mainly focuses on the economically developed regions such as Beijing-Tianjin-Hebei, Yangtze River and Pearl River Deltas (Tao et al., 2015; Han et al., 2015a, 2015b; Cui et al., 2016; Xia et al., 2017), while there have been few studies focusing on visibility in western China. Located in the Eurasian continental bridge economic belt, Urumqi is an important economic center in western China. With the sustained and rapid economic development, air pollution has become more and more severe. Moreover, Urumqi is surrounded by mountains and has arid climate (Turap et al., 2019), resulting in secondary inorganic ions and carbonaceous aerosols contribute largely to fine particle. The chemical species in $PM_{2.5}$ can affect atmospheric visibility. Therefore, it is crucial to study the relationship between the chemical composition of $PM_{2.5}$ and atmospheric visibility.

This study characterized daily $PM_{2.5}$ samples collected in the southern Urumqi during sep.2017 to aug.2018. And light extinction coefficients was estimated by IMPROVE formula. Multiple linear regression (MLR) was used to elucidate the correlation of visibility with the chemical components of $PM_{2.5}$. The sources of atmospheric extinction were also attributed with the Positive Matrix Factorization (PMF) model.

1. Experimental method

1.1. Sample collection

$PM_{2.5}$ samples were collected on the roof of No.9 building (43° 46′ 29″N, 87° 37′ 18″E) of Xinjiang University in Urumqi (Fig. 1). The sampling site was about 25 m high and is surrounded by residential, traffic and construction emissions and representative of urban Urumqi. $PM_{2.5}$ samples were collected from Sep. 2017–Aug. 2018. Daily 22-hr sampling from 10:00 a.m. to next day at 8:00 a.m. were carried out continuously for seven days every month. During each sampling episode, meteorological parameters, visibility and concentrations of gas contaminants were recorded (https://www.aqistudy.cn/). A blank sample was collected in each month. $PM_{2.5}$ samples were collected on quartz fiber filter (203 mm × 254 mm, Whatman, British). All filters wrap in aluminum foil and prebaked at 450 °C for 4 hr to remove absorbed organic material. $PM_{2.5}$ samples were collected using high-volume air sampler (TH-1000, Wuhan Tianhong instruments Co., Ltd, China) with a flow at 1.05 m^3/min. After each sampling, the filter wrap in the aluminum foil again and stored under −20 °C to prevent evaporation of volatilized components.

1.2. Gravimetric weighing

All filters were weighted before and after sampling to obtain particle mass concentrations by using electronic microbalance (AB204-S, Mettler Toledo, Switzerland) after 24 hr equilibration at 20 ± 2 °C and relative humidity at 45%–55%. Each filter was weighed at least three times before and after sampling respectively. The difference between replicate was not exceeding 0.00003 g. If not so, the filters would be equilibration for 24 hr and weighted again.

1.3. Chemical analysis

A punch of each $PM_{2.5}$ sample was placed into centrifuge tube and submerged in 10 mL of ultrapure water (18.2 MΩ/cm). Then an ultrasonic bath was operated for 20 min at low temperature (<10 °C), followed by centrifuge (11,000 r/min) for 10 min. The extract solutions were filtered with a polytetrafluoroethylene membrane (0.45 μm pore size), transferred into cleaned glass bottles, and then analyzed by Ion chromatography (883 Basic IC Plus, Metrohm, Switzerland) immediately. Five cations (Na^+, NH_4^+, K^+, Mg^{2+}, Ca^{2+}) and three anions (SO_4^{2-}, NO_3^-, PO_4^{3-}, Cl^-, F^-) were determined. In this study, the detection limits of Na^+, NH_4^+, K^+, Mg^{2+}, Ca^{2+}, SO_4^{2-}, NO_3^-, PO_4^{3-}, Cl^- and F^- are 0.014, 0.014, 0.046, 0.017, 0.041, 0.018, 0.032, 0.136, 0.022 and 0.026 μg/m^3, respectively. The recovery of each ion was 90%–105%.

A punch of 0.5 cm^2 from each filter was analyzed for OC and EC using DRI Model 2015 Thermal/Optical Carbon Analyzer (Desert Research Institute, USA), using the IMPROVE_A protocol to measure OC and EC (Chow et al., 2001). The method detection limits (MDLs) for the OC and EC were 0.05 $\mu g/m^3$, respectively. Replicate measurements were performed every ten samples, and the difference between replicate was < 10%.

1.4. IMPROVE equation

The IMPROVE formula reflects the relationship between the chemical composition of the aerosol and the atmospheric extinction (absorption and scattering). Assuming an externally mixed aerosol model consisting of large and small size modes, and the formula for calculating the extinction coefficient in urban atmosphere is as:

$$b_{ext} = b_{ap} + b_{sp} + b_{ag} + b_{sg} \quad (1)$$

where, b_{ap}, b_{sp} represent the absorption and scattering coefficients of aerosol, b_{ag} and b_{sg} absorption and scattering of gas, respectively.

$$b_{ap} = 10 \times [EC] \quad (2)$$

$$b_{sp}(\text{revised}) = 2.2 \times f_S(RH) \times [(NH_4)_2SO_4]_{small}$$

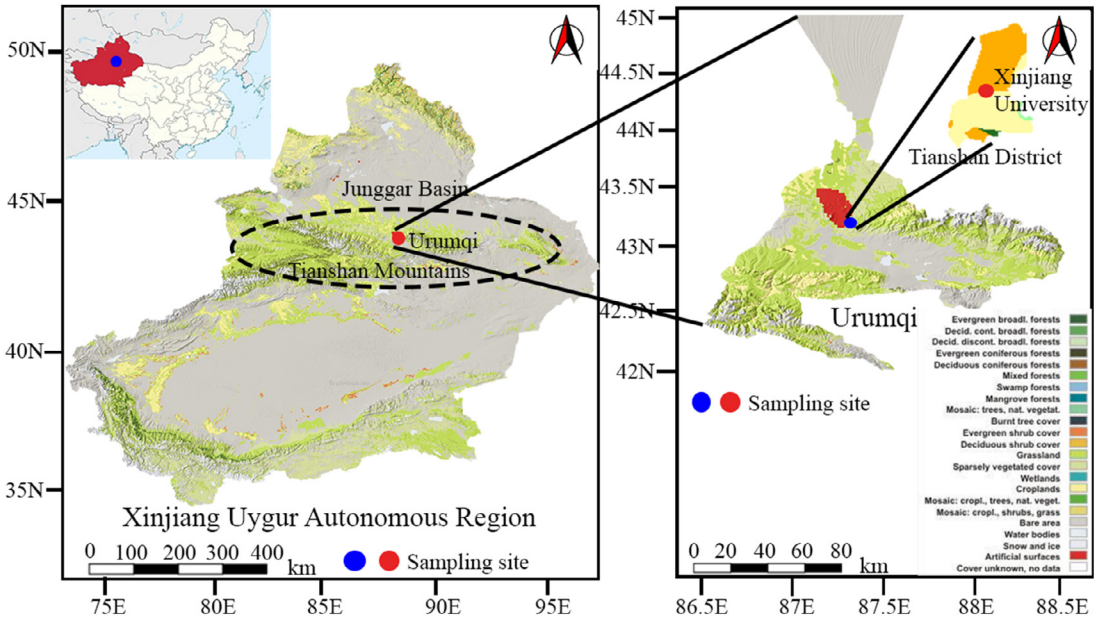

Fig. 1. – Location of sampling site.

$$+4.8 \times f_L(\mathrm{RH}) \times [(\mathrm{NH_4})_2\mathrm{SO_4}]_{large}$$
$$+2.4 \times f_S(\mathrm{RH}) \times [\mathrm{NH_4NO_3}]_{\mathrm{small}}$$
$$+5.1 \times f_L(\mathrm{RH}) \times [\mathrm{NH_4NO_3}]_{\mathrm{large}}$$
$$+2.8 \times [\mathrm{OM}]_{\mathrm{small}} + 6.1 \times [\mathrm{OM}]_{\mathrm{large}} + [\mathrm{finesoil}]$$
$$+0.6 \times [\mathrm{coarsematter}] \quad (3)$$

where, [large X] = [total X]^2/(20 μg/m^3), when [total X] < 20 μg/m^3;

[large X] = [total X], when the [total X] > 20 μg/m^3;

[small X] = [total X] - [large X]; here X refers to $(NH_4)_2SO_4$, NH_4NO_3 and OM concentrations.

$[(NH_4)_2SO_4] = 1.375[SO_4^{2-}]$; $[NH_4NO_3] = 1.29[NO_3^-]$ (Dan et al., 2017). Since the metal elements were not measured, fine soil was set to be 20 times Ca^{2+} concentration (Amato and Hopke, 2012). Due to the small contribution of coarse mass to extinction, we ignore them in this study (Hodkinson, 1966). f_S(RH) and f_L(RH) are hygroscopic growth factors (Pitchford et al., 2007). The gas extinction is mainly caused by NO_2, b_{ag} and b_{sg} (Rayleigh scattering of clear air) are 161[NO_2] and 10, respectively.

2. Results and discussion

2.1. Characteristic of PM2.5 and major species

Fig. 2 shows the concentrations of $PM_{2.5}$, water-soluble ions, OC and EC during the sampling period. $PM_{2.5}$ concentrations in the air of Urumqi largely exceeded the Chinese National air quantity standards (daily value of 75 μg/m^3 and annual value of 35 μg/m^3). The highest concentrations in fall and spring was 162.75 ± 80.04 μg/m^3, and 160.51 ± 91.46 μg/m^3, respectively. And the lowest $PM_{2.5}$ levels of 123.43 ± 36.83 μg/m^3 occurred in summer. SO_4^{2-} is the most abundant water-soluble ion (19.64 ± 20.14 μg/m^3), accounting for 17.48% ± 18.84% of $PM_{2.5}$ mass, followed by NO_3^- (18.25 ± 19.74 μg/m^3, 15.69% ± 16.72%) and NH_4^+ (12.66 ± 12.39 μg/m^3, 11.11% ± 11.25%). The dominance of the three ions was consistent with the previous results in Urumqi (Chen et al., 2014; Singh et al., 2017). The high

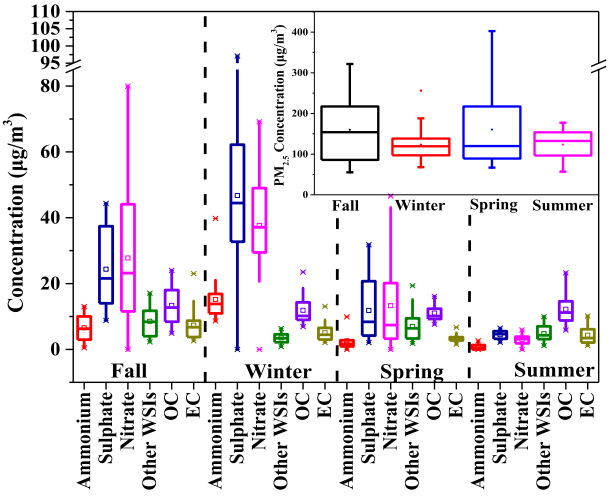

Fig. 2. – Seasonal variation of $PM_{2.5}$, water-soluble ions (WSIs), OC and EC during sampling period (The top down represents the maximum, upper quartile, median, lower quartile, and minimum, and the asterisk represents the outlier).

level of SO_4^{2-}, NO_3^- and NH_4^+ in heating period (November 2017 to March 2018) was likely owing to increase of anthropogenic emissions (i.e. vehicle exhaust and coal combustion) coupled with poor dispersion conditions (such as special topography, low wind speed and high RH). Other water-soluble ions (5.64 ± 3.87 μg/m^3) only contributed 2.54%–5.31% of $PM_{2.5}$ masses. On average, ten water-soluble ions together contributed 37.56% of $PM_{2.5}$ mass. The ten water-soluble ions were sorted by their mass during period of measurement: $SO_4^{2-} > NO_3^- > NH_4^+ > Ca^{2+} > Na^+ > F^- > Cl^- > PO_4^{3-} > K^+ > Mg^{2+}$. The ratio of AE/CE (Anion Equivalent/Cation Equivalent) value slightly lower than one, indicating the $PM_{2.5}$

Table 1. – Average RH and mass concentrations of SO_4^{2-}, NO^{3-} and NH_4^+ in different visibility range (Mean ± SD).

Range of Vis (km)	Average Vis (km)	SO_4^{2-}(μg/m^3)	NO_3^-(μg/m^3)	NH_4^+(μg/m^3)	Relative Humidity (%)
Vis < 4 (n = 22)	2.03 ± 0.92	54.64 ± 36.17	45.26 ± 30.21	17.04 ± 12.80	75.96 ± 8.16
4 < Vis < 7 (n = 25)	5.92 ± 0.93	17.86 ± 11.21	21.38 ± 21.17	4.07 ± 3.80	46.79 ± 19.65
7 < Vis < 9 (n = 33)	7.65 ± 0.34	5.56 ± 3.03	4.98 ± 4.97	0.92 ± 0.82	38.05 ± 11.03

Table 2. – Correlation matrix of atmospheric visibility verse components in the $PM_{2.5}$, RH and NO_2 gas concentration during sampling period.

	$PM_{2.5}$	NH_4^+	NO_3^-	SO_4^{2-}	NO_2	RH
Vis	0.024	−0.676**	−0.670**	−0.724**	−0.663**	−0.781**

** The correlation was significant at the 0.01 level; *: the correlation was significant at the 0.05 level.

aerosols were characterized by alkaline in nature during autumn, spring and summer seasons, while $PM_{2.5}$ aerosols were neutral in winter (Fig. 1**S**).

Carbonaceous aerosols were also the main component of $PM_{2.5}$. Assuming that organic matter (OM) is 1.6 times of OC (Turpin and Lim, 2001), total carbonaceous aerosols (TCA = EC + OM) accounted for 18.46%–20.17% of $PM_{2.5}$ mass. There was a good correlation between OC and EC, suggesting similar sources (i.e. vehicle exhaust, fossil fuel incomplete combustion and biomass burning (Cao et al., 2005)) (Fig. 2**S**). OC/EC ratios during this campaign period were in the range of 1.45 to 7.78 with a mean of 2.90. The OC/EC ratios in Urumqi were higher than those reported in the megacities in China (1.68–2.65) (Xiang et al., 2016), indicating substantial secondary organic aerosols in this area (Chow et al., 1994).

2.2. *Impact of SNA and RH on visibility*

To check the impact of $PM_{2.5}$ chemical composition on visibility, we categorized the visibility (Vis) data into three groups: Vis < 4 km (low-visibility), 4 km < Vis < 7 km (moderate-visibility), and 7 km < Vis < 9 km (high-visibility). The concentrations of SO_4^{2-}, NO_3^- and NH_4^+ in the low-visibility days were 9.8, 9.1 and 17.4 times higher than those in the high-visibility days, respectively (Table 1). Further analysis found that visibility decreased with the increases of SO_4^{2-}, NO_3^-, NH_4^+, NO_2 concentrations and RH (Table 2).

Fig. 3 presents the response of visibility with respect to $PM_{2.5}$, SNA (SNA = $[SO_4^{2-}]+[NO_3^-]+[NH_4^+]$) and RH. When RH was lower than 70%, the impact of SNA concentrations on visibility was significantly larger than that of $PM_{2.5}$. And visibility decrease was mainly bond up with SNA concentration. When RH was higher than 70%, visibility reduction was much more dramatic, indicating stronger influence of RH on visibility. Therefore, the attenuated visibility was primary due to the synergistic effect of SNA and RH.

There is a complex nonlinear relationship of visibility with SNA, RH. As Fig. 3 shows, visibility was negatively correlated with SNA. With an increase in the SNA mass concentration, visibility decrease exponentially. We further checked the relationship between visibility and SNA under different RH conditions: RH < 40%, 40% < RH < 70% and RH > 70%. The fitting curves were as follows:

RH < 40%, Vis = 9.40*[SNA]$^{-0.11}$ (R^2 = 0.45)
40% < RH < 70%, Vis = 10.80*[SNA]$^{-0.17}$ (R^2 = 0.67)
RH > 70%, Vis = 60.24*[SNA]$^{-0.67}$ (R^2 = 0.38)

At the 40% < RH < 70% conditions, visibility exhibited a strong dependence on SNA. And the correlations became weaker when RH was lower or higher. As shown in Fig. 4, the concentration of SNA at 100 μg/m^3 was a critical point. When the concentrations of SNA were higher than 100 μg/m^3, the variation of visibility was not apparent.

2.3. *Atmospheric extinction coefficient*

Based on the IMPROVE formula, we reconstructed atmospheric light extinction coefficient (b_{ext}) in Urumqi. As shown in Fig. 5, b_{ext} values were the highest in winter (1441.05 ± 739.95 Mm^{-1}), and the lowest in summer (128.58 ± 58.00 Mm^{-1}). $(NH4)_2SO_4$ and NH_4NO_3 were the major contributors, together accounting for 57.05% of the total b_{ext}. The contributions of carbon component, fine soil and gaseous contaminants to extinction coefficient were 30.19%, 10.3% and 2.46%, respectively (in Fig. 5). High mass fractions of sulfate and nitrate (SNA) in $PM_{2.5}$ and high RH (>70%) also occurred in winter, resulting in the largest b_{ext} contributions of $(NH4)_2SO_4$ and NH_4NO_3 reaching 87.54%. The proportion of total carbonaceous aerosol was the lowest in winter (10.53%) and the highest in summer (56.41%). The contribution of NO_2 to b_{ext} was the largest in summer. In Urumqi, NO_2 and SO_2 that are precursors of nitrate and sulfate mainly emitted from vehicles exhaust and coal combustion, respectively. In this study, the ratio of NO_3^-/SO_4^{2-} range from 0.68 to 1.22 with an average of 0.91, theoretically indicating that the contribution of stationary sources to total light extinction coefficient was slightly higher than that of mobile source during the investigated period.

Light extinction coefficient could be retrieved by Koschmieder formula ($b_{ext\text{-}v}$ = Ln ε / Vis, here ε is assumed to be 0.05) (Hinds, 1999). The average values of b_{ext} and $b_{ext\text{-}v}$ were 685.34, 967.92 Mm^{-1}, respectively. Although atmospheric b_{ext} values reconstructed by IMPROVE formula were about 29.19% lower than those by Koschmieder formula, the datasets by both methods were correlated well with each other (R^2 = 0.87, Fig. 5). The deviations might be introduced by the several influence factors as follows: 1) The atmospheric pollution in Urumqi is serious (especially the SNA) and high RH during winter (blue box); 2) In warm weather conditions, nitrate will decompose, resulting in the Light extinction coefficient was underestimated via revised IMPROVE formula (red box). In addition, the ε value used in this study might be overestimated since the value in Koschemieder equation would vary from place to place (Jiang et al., 2018).

2.4. *Correlation of visibility with light extinction coefficient*

There is a strong inverse correlation between b_{ext} and atmospheric visibility. The light scattering coefficients were dominated over light absorption coefficients, since SNA and OM levels were much higher than that EC. Fig. 6 presents the correlations of visibility with light scattering (b_{sp}) and light extinction coefficient (b_{ext}) during the sampling period. The fitting result is completely different from the Koschemieder's

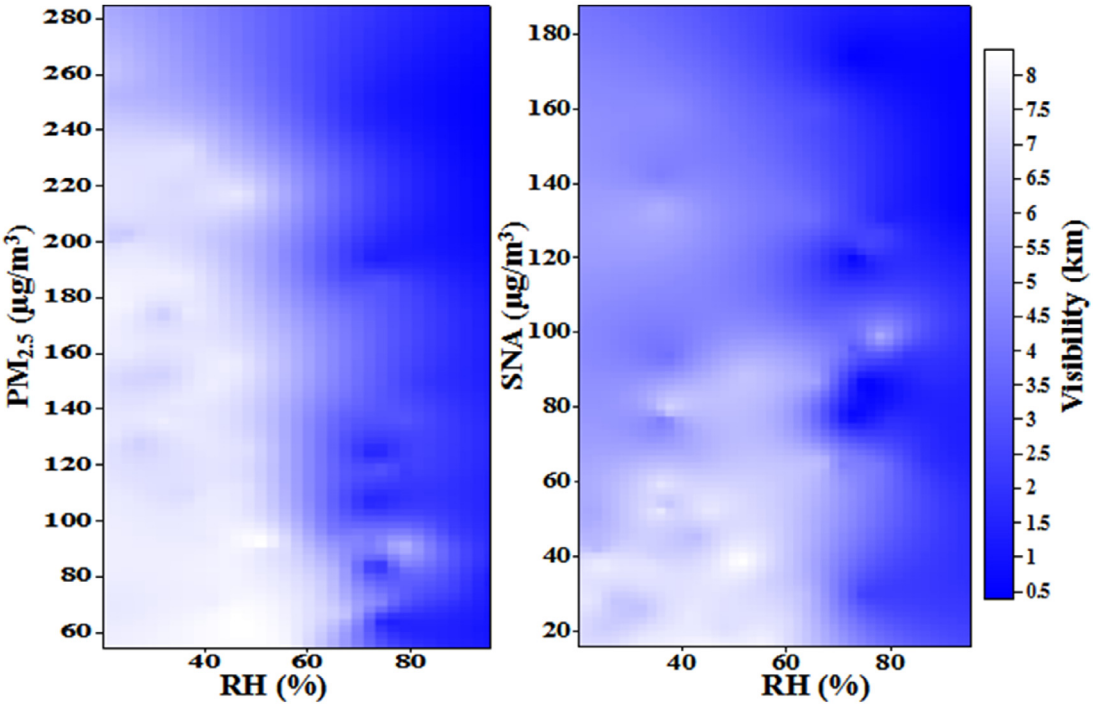

Fig. 3. – Image of mass concentration of $PM_{2.5}$ or SNA (SNA=[SO_4^{2-}]+[NO_3^-]+[NH_4^+]) concentrations, relative humidity on visibility.

equation in mathematical expression. The inverse relationship between Visbility and b_{sp} or b_{ext} still exists. The power of b_{sp} and b_{ext} in the two fitting formulas are 0.216 and 0.265, respectively, which are much lower than the those of b_{ext} in the Koschemieder's equation. The likely reason may be that the parameter settings in the IMPROVE equation are incompletion applicable to the southern atmosphere of Urumqi. Another reason is the Koschmieder's equation only applies to ideal observations (Dzubay et al., 1982).

Moreover, the multiple linear regression (MLR) method in R-3.6.0 and SPSS19 was further used to reconstruct the empirical regression model of visibility as a function of $(NH_4)_2SO_4$, NH_4NO_3, remaining amount of $PM_{2.5}$ ($PM_{2.5\text{-remainder}}$), NO_2 and RH. The results were listed in Table 3. The estimated regression coefficients in the visibility model were examined through *t*-test, and the *p*-values were less than 0.01 at the 95% confidence level. Although there was a difference between the two equations of linear fitting regression, a good correla-

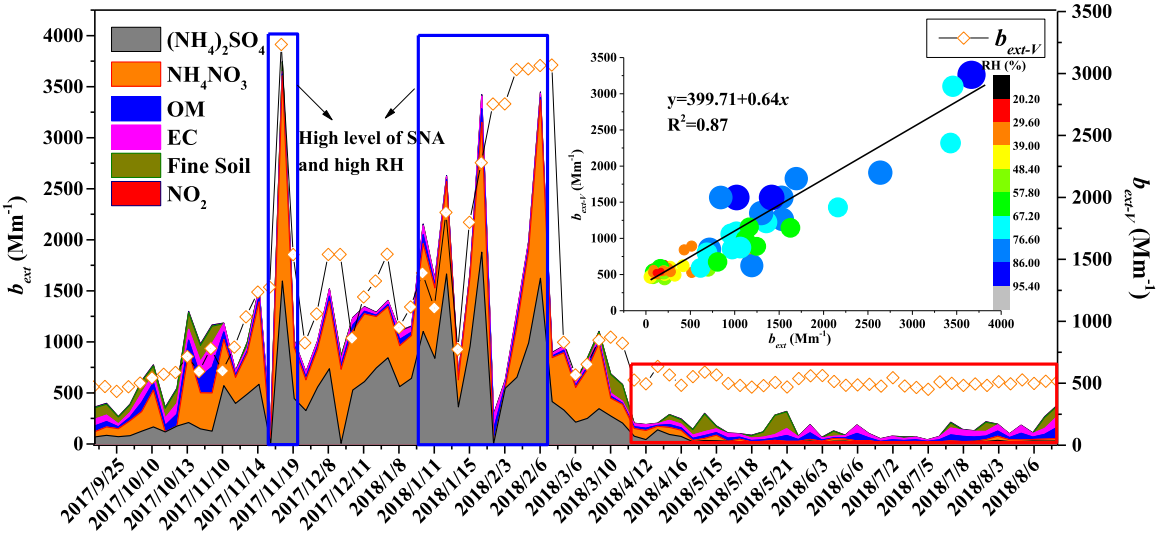

Fig. 5. – Temporal variations of light extinction coefficient via IMPROVE (b_{ext}) and Koschmieder's formulas ($b_{ext\text{-}v}$). The inset illustration represent the comparison of the b_{ext} and $b_{ext\text{-}v}$.

Table 3. – Multiple linear regression results by SPSS and R software for the empirical model of visibility in the Urumqi in sampling period (Vis = Constant + a1 × [$(NH_4)_2SO_4$] + a2 × [NH_4NO_3] + a3 × PM2.5-remainder + a4 × RH + a5 × NO_2).

	Parameter	Estimated regression coefficient (*a*)	Estimated standard deviation	*t* value	*p* value
Eq. (1)(Vis retrieved from MLR with SPSS, $R^2 = 0.822$)	Constant	10.863	0.585	18.573	0.000
	$(NH_4)_2SO_4$	−0.024	0.005	−4.432	0.000
	NH_4NO_3	−0.017	0.006	−2.796	0.007
	$PM_{2.5\text{-remainder}}$	−0.007	0.002	−3.369	0.001
	RH	−0.066	0.009	−7.491	0.000
Eq. (2)(Vis retrieved from MLR with R, $R^2 = 0.807$)	Constant	12.255	0.580	21.117	0.000
	$(NH_4)_2SO_4$	−0.024	0.005	−4.943	0.000
	$PM_{2.5\text{-remainder}}$	−0.008	0.002	−3.706	0.000
	NO_2	−0.028	0.007	−3.801	0.000
	RH	−0.078	0.008	−9.196	0.000

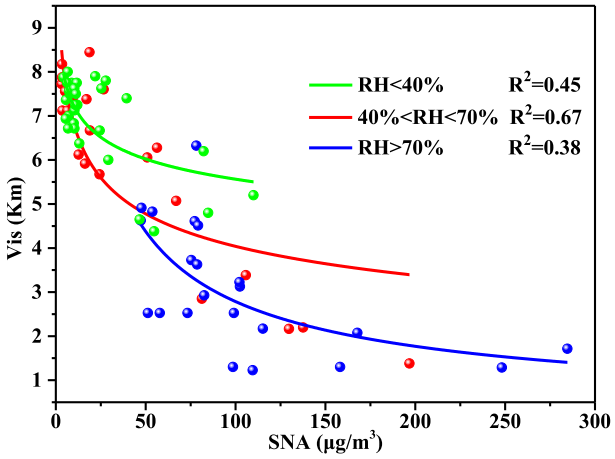

Fig. 4. – Scatter plot of the visibility and mass concentration of SNA.

tion was found between the reconstructed visibility and the measured visibility and the slope was close to one (Fig. 3S). This suggested that the two equations could reflect the relationship between visibility and atmospheric chemical components.

2.5. *Principal component analysis of visibility and cases analysis*

Atmospheric visibility is directly or indirectly affected by many interactional factors. To identify the major factors controlling the variation of visibility, principal component analysis (PCA) was conducted for the data during the observing period. The data of SO_4^{2-}, NO_3^-, NH_4^+, Ca^{2+}, OC, EC, RH, wind speed, surface pressure were input in the PCA. As Table 4 showed three main factors were identified by the PCA. All the three factors have statistically significant correlations ($p < 0.05$) with atmospheric visibility.

With the maximum explained variance (58.79%), the factor 1 had strong loading from SO_4^{2-} (0.684), NO_3^- (0.882), NH_4^+ (0.890), RH (0.791), WS (−0.672), pressure (0.843). This factor suggested that a stable and serious air pollution condition could result in low visibility. Low visibility from Nov 13, 2017 to Feb 7, 2018 was affected by this factor (Fig. 5). The second factor, explaining 30.10% of the variance, had high factor loading for OC (0.895) and EC (0.904), indicating that the variation of visibility was related with OC and EC. This factor reflected the influence of carbonaceous aerosols on visibility, especially during Jul 7 to 8 and Aug 1 to 8, 2018. With the explained variance of 11.11%, factor 3 characterized by Ca^{2+} (0.819). During

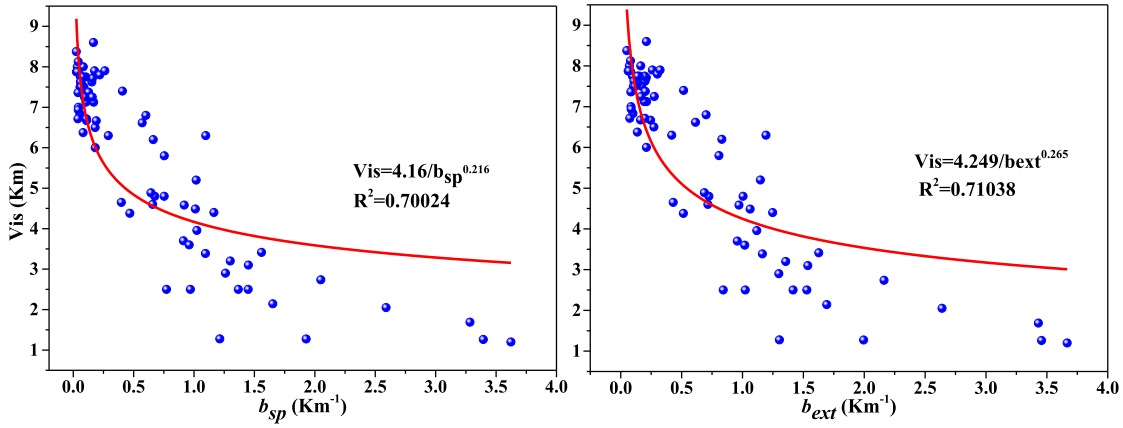

Fig. 6. – the relationship between scattering (b_{sp}) or light extinction coefficient (b_{ext}) and visibility during study period.

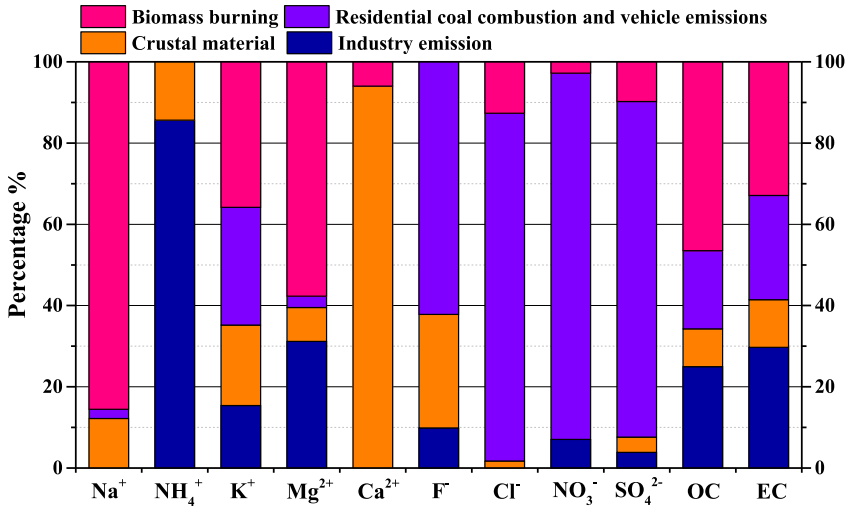

Fig. 7. – Source profile (%) obtained from PMF model analysis.

Table 4. – Factors loading from principal component analysis for the data in Urumqi during sampling period ($n = 80$, values in bold indicate loading factors larger than 0.5).

	Factor 1	Factor 2	Factor 3
SO_4^{2-}	**0.684**	0.360	−0.352
NO_3^-	**0.882**	0.121	0.226
NH_4^+	**0.890**	0.045	0.036
Ca^{2+}	−0.108	0.311	**0.819**
OC	−0.006	**0.895**	0.175
EC	0.146	**0.904**	0.095
Relative humidity	**0.791**	−0.230	−0.361
Wind speed	**−0.672**	−0.170	0.393
Pressure	**0.843**	0.031	−0.224
Variance (%)	58.79	30.10	11.11

May 18 to 21, 2018, the meteorological conditions were unstable and the sandstorms happened frequently, which significantly affected atmospheric visibility.

2.6. *Source contributions to light extinction*

Positive matrix factorization (PMF) model has been widely used in source apportionment. We used PMF model to estimate the contributions of aerosol sources that cause visibility deterioration. Data of WSIs (Na^+, NH_4^+, K^+, Mg^{2+}, Ca^{2+}, F^-, Cl^-, NO_3^-, SO_4^{2-}), OC and EC were used as input for the PMF model. Four main sources were identified, including residential coal combustion and vehicle emissions, industrial emission, crustal material and biomass burning (Fig. 7).

Factor 1 is characterized by high loadings of Cl^- (85.63%), SO_4^{2-} (82.62%) and NO_3^- (90.18%). Previous studies indicated that SO_4^{2-} and NO_3^- are formed through the oxidation of SO_2 and NO_x from coal combustion and vehicle exhaust, respectively (Zhang et al., 2013; Tao et al., 2014; Liu et al., 2017). Residential coal burning is an important source of $PM_{2.5}$ in Urumqi (Turap et al., 2019). So factor 1 related to residential coal combustion and vehicle emissions. Due to the lack of other specific indicators (such as V, As and PAHs), PMF cannot separate residential coal burning sources from vehicle exhaust, so treat them as one source. In this study, the contribution of residential coal combustion and vehicle emissions to light extinction was 58.6%, probably due to the high emissions of SO_2 and NO_x and strong oxidation in Urumqi during the winter (Zhang et al., 2017).

Factor 2 is dominated by NH_4^+ (85.64%), Mg^{2+} (31.18%), OC (24.96%) and EC (29.69%), which were closely related to industrial pollution (Wang et al., 2016; D. Wu et al., 2017; Zhou et al., 2016). The contribution of this source to the light extinction was 14.4%. Although Urumqi's air quality has improved in recent years, there are still many industrial zones around Urumqi, i.e. Midong-Wujiaqu industrial zone and coal-fired power plants.

Factor 3 is identified as crustal material on the basis of high leading of Ca^{2+} (94.02%) which are tracer compounds for crustal material (Zhang et al., 2013). The contribution of this source to the light extinction was 9.8%. Crustal material in Urumqi may originate from not only construction and re-suspended road dust, but also transported soil from Gobi Desert and Junggar Basin.

Factor 4 is distinguished by Na^+ (87.86%), K^+ (34.19%), Mg^{2+} (52.86%), OC (42.62%) and EC (31.50%) and associated with biomass burning (Zou et al., 2018). The contribution of biomass burning accounted for 17.2% of the light extinction. There are large agricultural areas in Xinjiang. The high contribution of biomass and waste burning should mainly come from the burning of straw during the harvest season.

Thus, residential coal combustion and vehicle emissions was the largest contributor to light extinction in Urumqi, followed by biomass burning, industry emission and crustal material (Fig. 8). Additionally, regional cooperation should be implement to improve the visibility by reduce emission from all pollution sources.

Acknowledgments

This work was supported by the National Natural Science Foundation of China (No. 41967050/41722305), the State Key Laboratory of Organic Geochemistry, GIGCAS (No. SKLOG-201915), the Guangdong Foundation for Program of Science and Technology Research (No. 2019B121205006), and the Local Innovative and Research Teams Project of Guangdong Pearl River Talents Program (No. 2017BT01Z134).

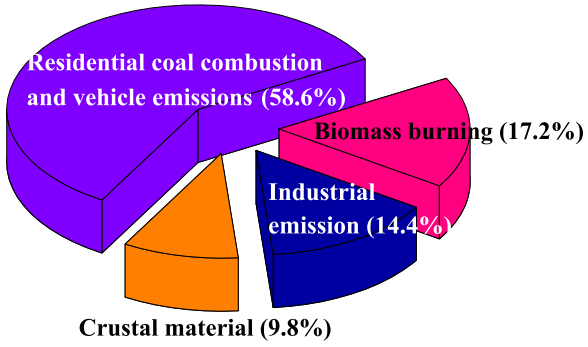

Fig. 8. – Source apportionment of the light extinction in south of Urumqi.

Appendix A. Supplementary data

Supplementary data associated with this article can be found in the online version Journal of Environmental Sciences at doi: 10.1016/j.jes.2020.07.007.

REFERENCES

Amato, F., Hopke, P.K., 2012. Source apportionment of the ambient pm2.5 across st. louis using constrained positive matrix factorization. Atmos. Environ. 46, 329–337.

Andreae, M.O., Gelencsér, A., 2006. Black carbon or brown carbon? The nature of light-absorbing carbonaceous aerosols. Atmos. Chem. Phys. 6 (10), 3131–3148.

Cao, J., Chow, J.C., Lee, S., Li, Y., Chen, S., An, Z., et al., 2005. . Characterization and source apportionment of atmospheric organic and elemental carbon during fall and winter of 2003 in Xi'an, China. Atmos. Chem. Phys. 5, 3127–3137.

Chen, J., Qiu, S., Shang, J., Wilfrid, O.M., Liu, X., Tian, H.Boman, et al., 2014. Impact of relative humidity and water soluble constituents of PM2. 5 on visibility impairment in Beijing, China. Aerosol Air Qual. Res. 14 (1), 260–268.

Chen, Y., Bond, T.C., 2009. Light absorption by organic carbon from wood combustion. Atmos. Chem. Phys. Discuss. 9 (5), 20471–20513.

Chow, J.C., Watson, J.G., Fujita, E.M., Lu, Z., Lawson, D.R., Ashbaugh, L.L., 1994. Temporal and spatial variations of PM2.5 and PM10 aerosol in the Southern California air quality study. Atmos. Environ. 28 (12), 2061–2080.

Chow, J.C., Watson, J.G., Crow, D., Lowenthal, D.H., Merrifield, T., 2001. Comparison of IMPROVE and NIOSH carbon measurements. Aerosol Sci. Technol. 34 (1), 23–34.

Cui, F., Chen, M., Ma, Y., Zheng, J., Yao, L., Zhou, Y., 2016. Optical properties and chemical apportionment of summertime PM2.5 in the suburb of Nanjing. J. Atmos. Chem. 73 (2), 119–135.

Dzubay, T.G., Stevens, R.K., Lewis, C.W., Hern, D.H., Courtney, W.J., Tesch, J.W., et al., 1982. Visibility and aerosol composition in Houston, Texas. Environ. Sci. Technol. 16 (8), 514–525.

Dan, W., Fan, Z., Xinlei, G., Meng, Y., Junrong, X., Gang, L., 2017. Chemical and light extinction characteristics of atmospheric aerosols in suburban Nanjing, China. Atmosphere (Basel) 8 (12) 149-.

Han, T., Qiao, L., Zhou, M., Qu, Y., Du, J., Liu, X., et al., 2015a. Chemical and optical properties of aerosols and their interrelationship in winter in the megacity Shanghai of China. J. Environ. Sci. 27, 59–69.

Han, T., Xu, W., Chen, C., Liu, X., Wang, Q., Li, J., et al., 2015b. Chemical apportionment of aerosol optical properties during the Asia-Pacific Economic Cooperation summit in Beijing, China. J. Geophys. Res. Atmos. 120 (23), 12281–12295.

Hand, J.L., Kreidenweis, S.M., Sherman, D.E., Collett Jr., J.L., Hering, S.V., Day, D.E., et al., 2002. Aerosol size distributions and visibility estimates during the Big Bend regional aerosol and visibility observational (BRAVO) study. Atmos. Environ. 36 (32), 5043–5055.

Hinds, W.C., 1999. Aerosol Technology: Properties, Behaviour and Measurement of Airborne Particles. Elsevier Ltd..

Hodkinson, J.R., 1966. Calculation of colour and visibility in urban atmospheres polluted by gaseous NO_2. Air Water Pollut. 10 (2), 137–144.

Jiang, L., Zhang, Z., Zhu, B., Shen, Y., Wang, H., Shi, S., et al., 2018. Comparison of parameterizations for the atmospheric extinction coefficient in Lin'an, China. Sci. Total Environ. 621, 507–515.

Jun, T., Tian-Tao, C., Ren-Jian, Z., 2015. Chemical composition of summertime PM2.5 and its relationship to aerosol optical properties in Guangzhou, China. Atmos. Ocean. Sci. Lett. 5 (2), 88–94.

Kaufman, Y.J., Tanré, D., Boucher, O., 2002. A satellite view of aerosols in the climate system. Nature (London) 419 (6903), 215–223.

Kim, K.W., Kim, Y.J., Oh, S.J., 2001. Visibility impairment during Yellow Sand periods in the urban atmosphere of Kwangju, Korea. Atmos. Environ. 35 (30), 5157–5167.

Liu, B., Wu, J., Zhang, J., Wang, L., Yang, J., Liang, D., Zhang, Q., 2017. Characterization and source apportionment of PM2.5, based on error estimation from EPA PMF 5.0 model at a medium city in China. Environ. Pollut. 222, 10–22.

Liu, Q., Wang, M.X., Zhang, R.J., 1999. Present research on atmospheric aerosol and its trends. China Powder Sci. Technol. 5 (3), 17–23 [In Chinese].

Lowenthal, D.H., Kumar, N., 2012. PM2.5 mass and light extinction reconstruction in IMPROVE. J. Air Waste Manage. Assoc. 53 (9), 1109–1120.

Palomo, A.O.L., 1999. Health 21: the health for all policy framework for the WHO European Region. J. Adv. Nurs. 30 (2), 280.

Pathak, R.K., Wu, W.S., Wang, T., 2009. Summertime PM2.5 ionic species in four major cities of China: nitrate formation in an ammonia-deficient atmosphere. Atmos. Chem. Phys Discuss. 9 (5), 1711–1722.

Pitchford, M., Malm, W., Schichtel, B., Kumar, N., Lowenthal, D., Hand, J., 2007. Revised algorithm for estimating light extinction from IMPROVE particle speciation data. J. Air Waste Manage. Assoc. 57 (11), 1326–1336.

Pope, C.A., Ezzati, M., Dockery, D.W., 2009. Fine-particulate air pollution and life expectancy in the United States. N. Engl. J. Med. 360 (4), 376–386.

Raizenne, M., Neas, L.M., Damokosh, A.I., Dockery, D.W., Spengler, J.D., Koutrakis, P., 1996. Health effects of acid aerosols on North American children: pulmonary function. Environ. Health. Persp. 104 (5), 506–514.

Singh, N., Murari, V., Kumar, M., Barman, S.C., Banerjee, T., 2017. Fine particulates over South Asia: review and meta-analysis of PM2.5 source apportionment through receptor model. Environ. Pollut. 223, 121–136.

Tan, J., Duan, J., Zhen, N., He, K., Hao, J., 2016. Chemical characteristics and source of size-fractionated atmospheric particle in haze episode in Beijing. Atmos. Res. 167, 24–33.

Tan, J., Zhang, L., Zhou, X., Duan, J., Li, Y., Hu, J., et al., 2017. Chemical characteristics and source apportionment of PM2.5, in Lanzhou, China. Sci. Total Environ. 601-602, 1743–1752.

Tao, J., Gao, J., Zhang, L., Zhang, R., Che, H., Zhang, Z., et al., 2014. PM2.5 pollution in a megacity of southwest China: source apportionment and implication. Atmos. Chem. Phys. Discuss. 14 (4), 5147–5196.

Tao, J., Zhang, L., Gao, J., Wang, H., Chai, F., Wang, S., 2015. Aerosol chemical composition and light scattering during a winter season in Beijing. Atmos. Environ. 110, 36–44.

Turap, Y., Rekefu, S., Wang, G., Talifu, D., Gao, B., Aierken, T., et al., 2019. Chemical characteristics and source apportionment of PM2.5 during winter in the southern part of Urumqi, China. Aerosol Air Qual. Res. 19 (6), 1325–1337.

Turpin, B.J., Lim, H.J., 2001. Species contributions to PM2.5 mass concentrations: revisiting common assumptions for estimating organic mass. Aerosol Sci. Technol. 35 (1), 602–610.

Wang, Q., Cao, J., Han, Y., Tian, J., Zhu, C., Zhang, Y., et al., 2018. Sources and physicochemical characteristics of black carbon aerosol from the southeastern Tibetan Plateau: internal mixing enhances light absorption. Atmos. Chem. Phys. 18 (7), 4639–4656.

Wang, Y., Jia, C., Tao, J., Zhang, L., Liang, X., Ma, J., et al., 2016. Chemical characterization and source apportionment of PM2.5 in a semi-arid and petrochemical-industrialized city, Northwest China. Sci. Total Environ. 573, 1031–1040.

Wu, D., Lin, S.L., Yang, H.Q., Du, R.G., Xia, J.R., Qi, B., et al., 2017a. Pollution characteristics and light extinction contribution of water-soluble ions of PM2.5 in Hangzhou. Environ. Sci. 38 (7), 2656–2666.

Wu, D., Zhang, F., Ge, X., Yang, M., Xia, J., Liu, G., et al., 2017b. Chemical and light extinction characteristics of atmospheric aerosols in suburban Nanjing, China. Atmosphere (Basel) 8 (8), 149.

Xia, Y., Tao, J., Zhang, L., Zhang, R., Li, S., Wu, Y., et al., 2017. Impact of size distributions of major chemical components in fine particles on light extinction in urban Guangzhou. Sci. Total Environ. 587-588, 240–247.

Zhang, R., Tao, J., Ho, K.F., Shen, Z., Wang, G., Cao, J., et al., 2012. Characterization of atmospheric organic and elemental carbon of PM2.5 in a typical semi-arid area of northeastern China. Aerosol Air Qual. Res. 12 (5), 792–802.

Zhang, R., Jing, J., Tao, J., Hsu, S.C., Wang, G., Cao, J., et al., 2013. Chemical characterization and source apportionment of PM 2.5 in Beijing: seasonal perspective. Atmos. Chem. Phys. Discuss. 13 (4), 9953–10007.

Zhang, J., Liu, L., Wang, Y., Ren, Y., Wang, X., Shi, Z., et al., 2017. Chemical composition, source, and process of urban aerosols during winter haze formation in Northeast China. Environ. Pollut. 231, 357–366.

Zhang, T., Cao, J.J., Tie, X.X., Shen, Z.X., Liu, S.X., Ding, H., et al., 2011. Water-soluble ions in atmospheric aerosols measured in Xi'an, China: seasonal variations and sources. Atmos. Res. 102 (1–2), 110–119.

Zhou, J., Xing, Z., Deng, J., Du, K., 2016. Characterizing and sourcing ambient pm2.5 over key emission regions in china i: water-soluble ions and carbonaceous fractions. Atmos. Environ. 135, 20–30.

Zhuang, B., Wang, T., Liu, J., Li, S., Xie, M., Han, Y., et al., 2017. The surface aerosol optical properties in the urban area of Nanjing, west Yangtze River Delta, China. Atmos. Chem. Phys. 17 (2), 1143–1160.

Zou, J., Liu, Z., Hu, B., Huang, X., Wen, T., Ji, D., et al., 2018. Aerosol chemical compositions in the North China Plain and the impact on the visibility in Beijing and Tianjin. Atmos. Res. 201, 235–246.